Surface Structure Determination from Scattering and Recoiling: W(211) and W(211)-$p(1\times2)$-O

J. W. Rabalais, O. Grizzi, M. Shi, and H. Bu
Department of Chemistry, University of Houston, Houston, Texas 77004-5641
(Received 16 January 1989)

Time-of-flight scattering and recoiling spectrometry with detection of both neutrals and ions for structure determinations is presented and applied to the clean W(211)-$p(1\times1)$ and W(211)-$p(1\times2)$-O structures. Experimental data are presented in the form of scattering and recoiling intensities versus beam incident angles and scattering and recoiling structural contour maps. The clean surface is relaxed both laterally and vertically from the bulk truncated structure. Oxygen atoms occupy threefold trough sites where they are bound to the two first-layer and one second-layer W atoms.

PACS numbers: 68.35.Bs, 79.20.Nc, 82.65.My

Low-energy (<10 keV) ion-scattering spectrometry[1] is one of the most actively developing surface science techniques due to important advances that have been recently realized.[2-6] This Letter describes time-of-flight scattering and recoiling spectrometry (TOF-SARS)[7] and applies it to determination of interatomic distances on clean W(211) and O_2 chemisorbed on W(211). It combines all of the recent advances, i.e., backscattering (BS), forwardscattering (FS), and direct recoiling (DR), TOF detection of both neutrals and ions, and continuous variation of the important angles. The result is a relatively nondestructive, highly sensitive, specific technique for structural analysis of both clean surfaces and adsorbate (including hydrogen) site positions.

TOF-SARS is based on the classical behavior of keV atom collisions where scattering occurs from the repulsive potentials of atomic cores, i.e., the nucleus plus core electrons. As a projectile ion approaches a target atom (Fig. 1), the trajectories are bent such that an excluded volume, i.e., a shadow cone, in the shape of a paraboloid is formed behind the target atom. Some of the deflected trajectories are focused at the edge of the cone. Since the radii of the cones are of the order of ~1 Å, the technique is extremely sensitive to the outermost atomic layers.

Scattering events.—When an ion beam is incident on a smooth surface at a grazing incident angle α, each surface atom is shadowed from the projectile ions by its neighboring atom such that only large impact-parameter (p) collisions are possible, resulting in FS. As α increases, a critical value $\alpha^1_{c,sh}$ is reached where the first-layer atoms move out of the cones; large-angle BS occurs when near head-on, i.e., $p\approx0$, collisions with first-layer atoms become possible. If the BS intensity I(BS) is monitored as a function of α, a steep rise (Fig. 1) with a well defined maximum is observed when the focused trajectories at the edge of the cone pass close to the centers of neighboring atoms. Increasing α still further leads to other $\alpha^2_{c,sh}$ values where subsurface-layer atoms move out of the first-layer atom cones. Rotating the crystal about the azimuthal angle δ aligns the beam with other crystal azimuths with different interatomic spacings, resulting in different $\alpha_{c,sh}$ values. Using a large scattering angle, i.e., $\theta>160°$, both the incoming and outgoing trajectories are similar, thus simplifying the geometry; this is the basis for impact-collision ion-scattering spectroscopy.[3] If the shape of the cone, i.e., the radius (R) as a function of distance (L) behind the target atom, is known, the interatomic spacing (d) can be directly determined.[2-7]

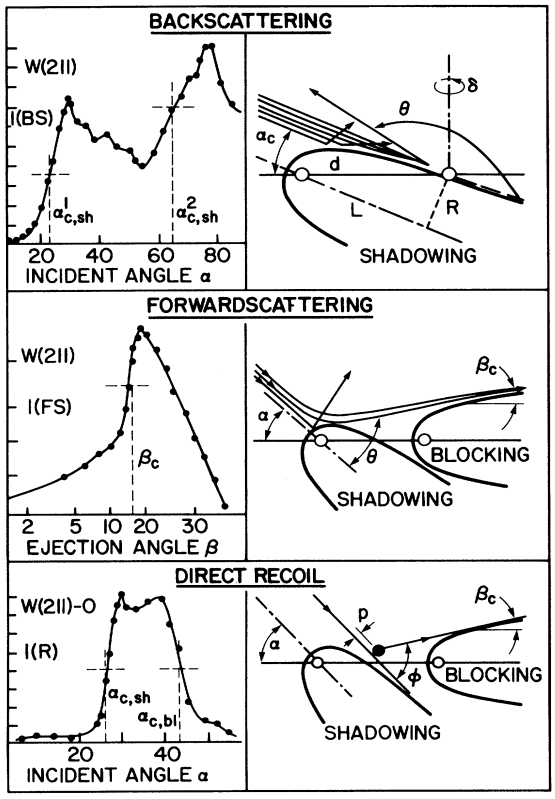

FIG. 1. BS, FS, and DR events observed in TOF-SARS along with representative plots for the W(211) surface of intensity vs α and β along the [$\bar{1}$11] azimuth. Open circles, W atoms. Closed circle, O atom.

For example, by measuring $\alpha_{c,\mathrm{sh}}^{1}$ along directions for which crystal azimuths are aligned with the projectile direction and using $d = R/\sin\alpha_{c,\mathrm{sh}}^{1}$, interatomic spacings in the first layer can be determined.

Recoiling events.— Light adsorbates can be efficiently detected[6-8] by recoiling them into a forward angle ϕ (Fig. 1). As α increases, the adsorbate atoms move out of their neighboring atom shadow cones so that direct collisions from incident ions are possible. When the p value necessary for recoil of the adsorbate atom into a specific ϕ becomes possible, adsorbate DR is observed. Focusing at the edge of the cones produces sharp rises in the DR intensities I(DR) as a function of α. By measuring $\alpha_{c,\mathrm{sh}}$ for the DR event, the interatomic distance from the adsorbate atom to its nearest neighbor can be directly determined[7] from p and the shape of the cone.

Blocking events.— There is a minimum ejection angle β (or $\alpha_{c,\mathrm{bl}}$) for both FS and DR below which atom trajectories are deflected by *blocking cones* of neighboring atoms (Fig. 1). Plotting I(FS) or I(DR) vs β results in a steep rise at β_c followed by a peak where the outgoing trajectories are focused onto the cone edge. Interatomic spacings can also be determined[7] from β_c and the shape of the cone.

The scattered and recoiled atoms can be identified by their TOF because they have high, discrete velocity distributions at specified θ and ϕ which are well described[6] by classical mechanics.[9,10] A TOF-SARS spectrometer[7] has been constructed which allows continuous variation of θ and ϕ with a flight path of 98.4 cm. It uses a pulsed, mass selected ion-beam source, a channel electron multiplier detector which is sensitive to both ions and fast neutrals, and standard timing electronics.[6] Typical experimental parameters are the following: 2–5-keV He^+, Ne^+, or Ar^+ pulsed primary beam; pulse width, 20–100 nsec; pulse rate, 10–50 kHz; average current density, 0.05–0.1 nA/mm^2; signal detection rate up to ≈ 30000 counts/sec. A TOF spectrum can be acquired in ≈ 20 sec with a dose of $\approx 10^{-4}$ ion/target atom. The W surface was cleaned by heating to 2300 K. Oxygen was chemisorbed as the surface approached room temperature using a saturation dose, after which a $p(1\times2)$ LEED pattern with a coverage of 1.5 monolayers[11-14] was observed.

Although structural data can be derived directly from experimental measurements alone, maximum information is obtained from the shape of the shadowing and blocking cones[9,10] or a simulation of the BS flux distributions.[4] Classical trajectory simulations[9,10] are used to trace the trajectories and map out the cones. Higher accuracy is achieved by calibrating the potential; this involves measuring α_c values along different azimuths for which d are accurately known and using these values to determine the experimental R at different L values. The screening constant is then adjusted for good agreement of the calculated cone and the experimental R and L points.

The data for structural analysis will now be considered. TOF-SARS spectra: Both BS and FS spectra[6] are collected and I(BS), I(FS), and I(DR) are determined as a function of α and δ. Incident angle α scans: Collecting I(BS) data as a function of α probes the ability of ions to make a direct hit ($p \approx 0$) on substrate atoms in various surface layers. Collecting I(DR) as a function of α and β probes, respectively, the ability of (i) incident ions to hit adsorbate atoms ($\alpha_{c,\mathrm{sh}}^{1}$), i.e., the entrance channel, and (ii) recoiling adsorbate atoms to escape from the surface ($\alpha_{c,\mathrm{bl}}$), i.e., the exit channel. Azimuthal angle δ scans: Collecting I(BS) as a function of δ illustrates (i) the symmetry of surface layers and (ii) the ability to directly view first and subsurface layers. Collecting I(DR) as a function of δ illustrates (i) the symmetry of adsorbate positions and (ii) azimuths along which the DR channel is accessible or obstructed.

Data for the clean and O_2 chemisorbed W(211) surface are given as scattering and recoiling structural con-

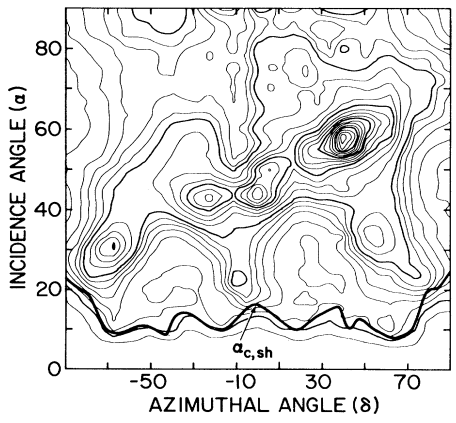

FIG. 2. SSCM for the clean W(211)-$p(1\times1)$ surface using 4-keV Ar^+ ions at a scattering angle $\theta = 163°$. Regions with high contour densities represent maxima in I(BS).

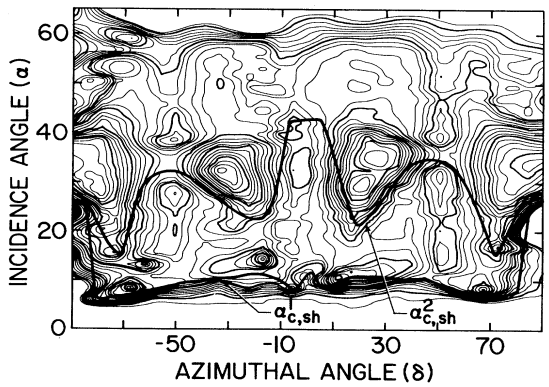

FIG. 3. RSCM for the W(211)-$p(1\times2)$-O structure using 4-keV Ar^+ ions at a recoiling angle $\phi = 65°$. Regions with high contour densities represent maxima in I(DR).

tour maps (SSCM and RSCM) in Figs. 2 and 3. These represent I(BS) and I(DR) data in (α,δ) space; contour lines connect points of equal intensity. The W(211) surface consists of parallel close-packed rows separated by wide channels (Fig. 4). These maps provide the following information: (i) They are a concise summary of the experimental BS and DR data. (ii) They show what regions of (α,δ) space contain interesting structures for closer, more detailed investigation. (iii) Since anisotropies in I(BS) are determined by crystal structure, SSCM's of clean surfaces reveal the symmetry of the data in (α,δ) space, providing a *fingerprint for a specific crystal face and type* with minor perturbations due to relaxation and possible major perturbations due to reconstruction. For light adsorbate covered surfaces, single BS events occur only from heavy substrate atoms, although the presence of light adsorbates near the trajectories cause small deflections; comparison of the SSCM's from the clean and adsorbate covered surfaces reveals the regions of (α,δ) space that are different and thereby indicate adsorbate site positions. Upon adsorption, alteration of the clean surface SSCM symmetry pattern along azimuths for which the trajectories do not intersect the adsorbate atom cones signals adsorbate-induced reconstruction. (iv) Since anisotropies in I(DR) are determined by the adsorbate site positions, RSCM's reveal the symmetry of DR data in (α,δ) space, providing a *fingerprint for an adsorbate at a specific coverage on a specific crystal face and type.*

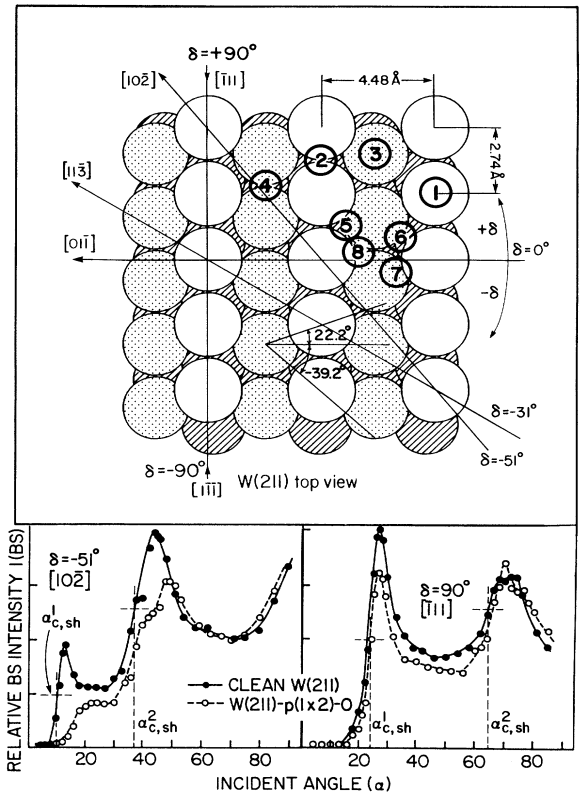

FIG. 4. Top: Adsorbate sites on the W(211) surface. The atomic sizes are scaled to the covalent radii of oxygen and tungsten. Interatomic spacings for the bulk truncated surface are indicated. The adsorption sites are defined as follows: (1) On-top and (2) bridging row sites, (3) on-top and (4) bridging trough sites, (5) threefold trough sites, and (6)–(8) asymmetrical trough sites. Bottom: Examples of I(BS) vs α at $\theta = 163°$ for two azimuths δ of the clean and $p(1\times2)$-O surface. The large $\alpha^1_{c,sh}$ shift ($\sim 8°$) along [10$\bar{2}$] is due to O atom perturbation of the Ar trajectories. The small shift (3°–4°) in the second peak and $\alpha^2_{c,sh}$ along [10$\bar{2}$] is due to interference of the O atom with second-layer scattering.

Consider details of the clean W(211) SSCM. The $\alpha^1_{c,sh}$ values correspond to shadowing of first-layer atoms by their first-layer neighbors; this line is symmetrical about $\delta = 0°$, as is the first layer. Intense structures are observed as α increases above 20° due to focusing and channeling of ion trajectories by first- and second-layer W atoms onto third- and fourth-layer W atoms and back out again. The asymmetry about $\delta = 0°$ is due to the lack of a mirror plane through the $\delta = 0°$ azimuth. A line of intense peaks runs diagonally from $\alpha \approx 30°$, $\delta \approx -70°$ towards $\alpha \approx 75°, \delta \approx +80°$. The diagonal orientation[7] results from focusing onto subsurface layers for $\delta < 0°$ at low α and $\delta > 0°$ at high α. For example, the lines through a second- and two adjacent first-layer W atoms (Fig. 4) are at $\delta = +22.2°$ and $-39.2°$; the shorter interatomic distance for $+22.2°$ requires higher α values for second-layer scattering, whereas such scattering occurs at lower α values for the longer distance at $-39.2°$.

The values of $\alpha^1_{c,sh}$ vs δ (Fig. 2) are consistent with first-layer interatomic distances which correspond to the bulk truncated W(211) structure; i.e., there is no reconstruction (no missing or buckled rows). It is, however, relaxed, i.e., a (1×1) reconstruction,[11] as detailed elsewhere.[7] Briefly, relaxation is determined from the $\alpha^2_{c,sh}$ values as follows. Lateral relaxation: I(BS) vs α scans along several azimuths δ centered near the position for which first- and second-layer atoms are expected to be aligned are measured. The δ which gives the maximum $\alpha^2_{c,sh}$ for second-layer scattering corresponds to the shortest distance between first- and second-layer atoms, thereby revealing the first- and second-layer alignment. For a bulk truncated surface, the first- and second-layer neighbors would be aligned for $\delta = 22.2°$ and $-39.2°$, while the maximum $\alpha^2_{c,sh}$ values occur at $\delta = 24.0°$ and $-37.5°$. Using these values, the first- and second-layer registry can be calculated, with the result that the lateral spacing from a second- to a first-layer atom along the [$\bar{1}$11] direction is 1.72 ± 0.07 Å, i.e., a shift of 0.11 ± 0.07 Å (6.0%) from the bulk value of 1.83 Å. Vertical relaxation: The maximum $\alpha^2_{c,sh}$ values for first- and second-layer scattering measured above are 29.1° ($\delta = 24.0°$) and 38.0° ($\delta = -37.5°$), the shapes of the

shadow cones are calculated,[7,10] and $p=0.037$ Å for $\theta=165°$. Using these data, the first- and second-layer spacing was found to be 1.17 ± 0.07 Å, i.e., contracted by 0.12 ± 0.07 Å (9.3%) from the bulk value of 1.29 Å. These results are in agreement with LEED data[11] which suggests that the first atomic layer is relaxed 0.09 Å parallel to and 0.16 Å perpendicular to the surface.

Consider the W(211)-$p(1\times2)$-O structure.[12] When the SSCM of the $p(1\times2)$-O structure is compared[7] to that of clean W(211), the same symmetry pattern as Fig. 2 is observed (indicating no adsorbate-induced reconstruction). However, the $\alpha^2_{c,\mathrm{sh}}$ values are larger than those of the clean surface by 3°–4° *along all* δ (with the exception of $\delta=\pm90°$), even for azimuths where the ion trajectories are far from the oxygen sites. This 3°–4° shift is consistent with reversion of the clean relaxed W(211) structure to the bulk truncated structure upon adsorption.

Of the possible oxygen adsorption sites indicated in Fig. 4, the only one that is consistent[7] with all of the experimental data is the threefold through site (site 5). The approximate symmetry of the RSCM (Fig. 3) about $\delta=0°$ indicates that the sites are symmetrical about this azimuth, thus eliminating sites 3, 4, 6, 7, and 8. The lack of perfect symmetry is due to variations in the measurements which were made over a period of several days. Examples of Ar I(BS) vs α scans for the clean and $p(1\times2)$-O surface are shown in Fig. 4. The lack of perturbation of I(BS) along $\delta=90°$ indicates that O is not close to the Ar BS trajectories, thus eliminating sites 1, 2, 3, and 4. The shift in $\alpha^1_{c,\mathrm{sh}}$ of 8° towards higher α along the $[10\bar{2}]$ azimuth indicates that O atoms interfere with BS trajectories and that higher α values are necessary to avoid the O atoms and obtain first-layer W atom BS. This 8° shift is consistent[7] with O atoms in site 5 at a height of ~0.5 Å above the first-layer W atom. The change in shape of the second peak indicates that O atoms on both the near and far sides of the troughs interfere with incoming and outgoing second-layer scattering trajectories, respectively, along this azimuth. This site is symmetric about the $\delta=0°$ azimuth and sufficiently far from Ar BS trajectories along $\delta=90°$ to cause no perturbations. This result agrees with one of the proposed LEED models,[12] the other models[13,14] suggesting sites 2 and 4. In site 5 the O atoms are bound[12] to two first-layer and one second-layer W atoms; these site coordinates and O–W bond lengths can be determined[7] to 0.1 Å.

The results show that the clean W(211) surface is relaxed and that oxygen atoms occupy threefold sites and revert the surface back to the bulk structure. The advantages of TOF-SARS are the following: (i) The high sensitivity and accuracy allows direct measurements of surface and adsorbate (including hydrogen) interatomic spacings which are independent of ion-surface neutralization problems and are relatively nondestructive due to detection of both neutrals and ions and to the efficient multichannel TOF mode. (ii) The SSCM and RSCM reveal the substrate and adsorbate symmetries in (α,δ) space. (iii) Surface- and subsurface-layer scattering structures can be delineated. (iv) Simple shadowing and blocking cone and trajectory simulations are adequate for interpretation of the structures. Details of the analysis of the W(211) relaxed structure and the adsorption coordinates for O_2 and H_2 chemisorption will be presented elsewhere.[7]

The authors are grateful to R. R. Rye (Sandia Laboratories) for providing the W(211) crystal and for many helpful discussions. This material is based on work supported by the National Science Foundation under Grant No. CHE-8814337 and the Texas Advanced Research Program.

[1]D. P. Smith, J. Appl. Phys. **38**, 340 (1967).

[2]For a recent review, see Th. Fauster, Vacuum **38**, 129 (1988).

[3]M. Aono and R. Souda, Jpn. J. Appl. Phys. **24**, 1249 (1985).

[4]J. A. Yarmoff, D. M. Cyr, J. H. Huang, S. Kim, and R. S. Williams, Phys. Rev. B **33**, 3856 (1986); J. H. Huang and R. S. Williams, Phys. Rev. B **38**, 4022 (1988); Surf. Sci. **204**, 445 (1988).

[5]L. Marchut, T. M. Buck, G. H. Wheatley, and C. J. McMahon, Jr., Surf. Sci. **141**, 549 (1984).

[6]J. W. Rabalais, CRC Crit. Rev. Solid State Mater. Sci. **14**, 319 (1988).

[7]O. Grizzi, M. Shi, H. Bu, J. W. Rabalais, and P. Hochmann (to be published).

[8]B. J. J. Koleman, S. T. de Zwart, A. L. Boers, B. Poelsema, and L. K. Verheij, Phys. Rev. Lett. **56**, 1152 (1986).

[9]E. S. Mashkova and V. A. Molchanov, *Medium Energy Ion Reflection from Solids* (North-Holland, Amsterdam, 1985); J. F. Zeigler, J. P. Biersack, and U. Littmark, *The Stopping and Range of Ions in Solids* (Pergamon, New York, 1985).

[10]S. R. Kasi, M. A. Kilburn, H. Kang, J. W. Rabalais, L. Tavernini, and P. Hochmann, J. Chem. Phys. **88**, 5902 (1988).

[11]H. L. Davis and G.-C. Wang, Bull. Am. Phys. Soc. **29**, 221 (1984).

[12]J. B. Benziger and R. E. Preston, Surf. Sci. **151**, 183 (1985).

[13]G.-C. Wang, J. M. Pimbley, and T.-M. Lu, Phys. Rev. B **31**, 1950 (1985); J. Vac. Sci. Technol. A **4**, 1357 (1986).

[14]J. F. Wendelken, J. Vac. Sci. Technol. A **6**, 662 (1988).